Isoform-specific NADPH oxidase inhibition for pharmacological target validation

V.T. Dao[a*], S. Altenhöfer[a]*, M.H. Elbatreek[a,b], A.I. Casas[a], P. Lijnen[a], M.J. Meens[a], U. Knaus[c], H.H.H.W. Schmidt[a]

[a] Department for Pharmacology and Personalised Medicine, FHML, Maastricht University, Maastricht, The Netherlands;

[b] Department of Pharmacology and Toxicology, Faculty of Pharmacy, Zagazig University, Zagazig, Egypt;

[c] Conway Institute, University College Dublin, Belfield, Dublin, Ireland

[*]Both authors contributed equally

Corresponding Author: Prof Harald Schmidt, Department for Pharmacology and Personalised Medicine, FHML, Maastricht University, PO Box 616, 6200 MD Maastricht, the Netherlands, Phone: +61-3-9905-5752; Email: h.schmidt@maastrichtuniversity.nl

Abstract

Unphysiological reactive oxygen species (ROS) formation is considered an important pathomechanism for several diseasephenotypes with high unmet medical need. After the clinical failure of antioxidants, inhibition of disease-relevant enzymatic sources of ROS appears to be the most promising alternative approach. With respect to most promising drug target, NADPH oxidases (NOXs) stand out, however, validation has been restricted mainly to genetically modified mice. Validation in other species including human is lacking and it is unclear whether the different NOX isoforms are sufficiently distinct for selective pharmacological inhibition. Here we show for the five most advanced NOX inhibitors that pharmacological isoform selectivity can be achieved. NOX1 was most potently (IC_{50}) targeted by ML171 (0.1 µM); NOX2, by VAS2870 (0.7 µM); NOX4, by M13 (0.01 µM) and NOX5, by ML090 (0.01 µM). Of note, previously unrecognised non-specific antioxidant and assay artefacts may limit interpretations in some systems, which included, surprisingly, the clinically most advanced compound, GKT136901. As proof-of-principle for our pharmacological target validation approach, we used a human blood-brain barrier model and our NOX inhibitor panel at IC_{50} concentrations. Indeed, the protective efficacy pattern of this compound panel pointed towards a functional role NOX4 confirming previous genetic targeting. These findings strongly encourage further lead optimisation efforts for isoform-selective NOX inhibitors and their clinical development and provide already now an experimental alternative when genetic targeting of NOXs is not an option.

Introduction

Reactive oxygen species (ROS) are considered an important pathomechanism for several common diseases with high unmet medical need including cardiovascular and neurodegenerative diseases as well as cancer. Yet, clinical translation of this hypothesis by therapeutic or even prophylactic use of antioxidants that scavenge ROS has consistently failed [1], in some cases even increasing mortality [2,3] [4].This paradox was initially explained by these compounds being possibly underdosed, thereby not reaching efficacy, or over being overdosed causing reductive stress.

It is now understood, however, that ROS are by no means only harmful metabolic by-products, but also serve important protective, metabolic and signaling functions, such as the regulation of cell proliferation, differentiation, migration and survival, innate immune response, vascular tone, neuronal signaling as well as inflammation [5-8]. Anti-oxidants will always simultaneously interfere with both qualities of ROS, the physiological and pathophysiological ones, and the overall neutral or deleterious outcomes of antioxidant studies likely show that the predominant quality of ROS is protective. Thus, ROS should not be interfered with in a systemic manner, but rather by identifying for each disease condition the relevant ROS source and inhibit by classical pharmacology, i.e. enzyme inhibition [9].

Of all potential sources of ROS, NADPH oxidases (NOX) stand out as they are the only known dedicated, evolutionary conserved ROS-forming enzyme family. Relevant dysregulation has been suggested for NOX1, contributing to diabetic atherosclerosis [10] and retinopathy [11]; NOX2, to neurodegeneration [12] but being protective in diabetes [10]; NOX4, to stroke [13], diabetic nephropathy [14] and neuropathic pain [15], but being protective in diabetic atherosclerosis [16,17]; and NOX5, in diabetic nephropathy[18,19], hypertension [20] and coronary artery disease[21].

Target validation of these NOX isoforms in different disease models has been done primarily by gene knock-out (as reviewed in [22]) and, in the case of NOX5 [18], by knock-in technology limiting most data sets to mice and, in the case of NOX4, in addition to rat [13]. For ultimate clinical translation and target validation in other species, NOX-specific and ideally isoform-selective NOX inhibitors are desirable. It is unclear, however, whether this is pharmacologically achievable given the fact that all five relevant NOX isoforms (NOX1, NOX2, NOX3, NOX4 and NOX5) are similarly structured transmembrane proteins containing conserved heme, FAD and NADPH binding sites. Some degree of functional variability derived from the fact that some isoforms have more (NOX1 and NOX2) or less (NOX4 and NOX5) binding partners or a unique calcium binding domain (NOX5) [23]. In addition, all ROS based activity assays are indirect opening the possibility that any compound exerts some of its apparent effects on ROS formation by direct ROS scavenging [24,25]) or direct assay interference [26,27].

Here, we examine some of the best characterized or most widely used NOX inhibitors, VAS2870, ML171, GKT136901, M13 and ML090. We first analysed the isoform selectivities, then possible assay interference and direct ROS-scavenging capacity, and finally suggest a NOX inhibitor panel for pharmacological target validation, which we then validate an *in vitro* human model of brain ischemia to identify NOX4 as a therapeutic target.

Material and Methods

Chemicals and reagents

Dulbecco's modified Eagle medium with GLUTAMAX (DMEM), RPMI-1640 medium with L-Glutamine and Hanks' buffered salt solution (HBSS) were purchased from GIBCO/Life Technologies. Fetal bovine serum (FBS), 2-Acetylphenothiazine (ML171), 5,12-Dihydroquinoxalino(2,3-B)quinoxaline (ML090), phorbol myristate acetate (PMA), calcein, diphenyleneiodonium chloride (DPI), dextran sulfate, dimethyl sulfoxide (DMSO), Luminol, sodium salt, superoxide dismutase (SOD), G418, ionomycin calcium salt ready to made solution and Penicillin/Streptomycin solution were purchased from Sigma–Aldrich. 3-Benzyl-7-(2-benzoxazolyl) thio-1,2,3-triazolo [4,5-di] pyrimidine (VAS2870) was provided by Vasopharm; the pyrazolopyridine derivative GKT 136901, by GenKyoTex; M13, by Glucox Biotech. Amplex Red and horseradish peroxidase (HRP) were purchased from Invitrogen, CA, USA. The FuGENE6 transfection reagent was purchased from Promega.

Cells

HEK293 cells were either stably or transiently transfected with human NOX01 (Gene ID: 124056), NOXA1 (Gene ID: 10811) and NOX1 (Gene ID: 27035) to measure NOX1 activity or individually with human NOX4 (Gene ID: 50507) or NOX5 (Gene ID: 79400) plasmids. All plasmids were confirmed by sequencing. Stable expression was reached by single clone selection from cells growing under selection medium containing 200 µg/ml G418. Briefly, FuGENE6 transfection reagent (Promega) was used in a ratio 4:1 with pcDNA3.1 DNA plasmid containing the sequence for either NOX 1, NOXO1, NOXA1 (triple transfection), NOX4 or NOX5. After removal of DMEM medium 240 µl of serum free medium was added to polystyrene tube followed by 10 µl of FuGENE directly into the medium and incubated for 5 min. at room temperature. Thereafter pre-

mixed DNA was added to the tube and incubated for 30 min. at room temperature. 250 µl of the mixture was added to the HEK293 cells. Selection was started after three days by changing to DMEM medium containing 200 µg/ml G418. The medium was changed every two to three days before a single clone has been selected. After trypsinisation and dilution a cell suspension of 27 cells/µl was used to prepare a single cell suspension of 1 µl pre-dilution in 12 ml HEK selection medium. Finally, 500 µl of single cell suspension per well seeded in 24-well plate.

In some experiments, HEK293 cells were transiently transfected with NOX4 or NOX5 or were triple transfected with NOX1, NOXO1 and NOXA1 using FuGENE6 followed by ROS measurement after 48h. As described previously[28], $O_2^{\bullet-}$ was measured in HL-60 cells (human, promyeloblast, ATCC-No.CCL 240) that were cultured in RPMI-1640 medium with 5% FCS (JRH Biosciences), penicillin (100 U•mL-1), streptomycin (100 µg•mL-1) and glutamine (2 mM). Cell suspensions (26 x 10^6 cells•mL-1) were incubated with 1.25% DMSO per 75cm^2 TCF for 7 days to induce differentiation into granulocyte-like cells that were then centrifuged at 300xg, washed with HBSS and re-suspended in HBSS to the final seeding density needed for the experiment (5 x 10^5 cells/well in 96 well plate).

ROS measurement in intact cells

H_2O_2 production was measured in intact cells using Amplex Red fluorescence. For the measurement, native HEK293 cells or HEK293 cells stably or transiently transfected with NOX4 or NOX5 were trypsinized, counted, washed and re-suspended in Krebs-Ringer-Phosphate Glucose buffer (KRPG). NOX inhibitors dissolved in DMSO or solvent control (0.5% DMSO) were added to respective wells of a black 96-well plate and 50 µl of a reaction mixture containing 0.1 U·mL-1 HRP and 50 µM Amplex Red was added to each well according to the kit manual and incubated at 37°C for 10 min. Thereafter, 100,000 of respective HEK293 cells or solvent control in 50 µl of KPRG-buffer were added to each well. Amplex Red fluorescence was measured immediately at

excitation (530-560 nm) and emission ~ 590 nm at 37ºC for 60 min. HEK293 cells expressing NOX5 were activated by the Ca^{2+} ionophore ionomycin (40 µM). Cells expressing NOX1 or NOX2 were activated with 2 µM Phorbol 12-myristate 13-acetate (PMA; PKC activator). $O_2^{\bullet-}$ production in HL-60 cells was measured by cytochrome C reduction as described previously [28]. Briefly, cytochrome C (100 µM) was added to the DMSO-differentiated HL-60 cell suspension. After adding 5 x 10^5 cells to a 96-well plate and addition of inhibitors, a basal reading was performed at 540 nm (isosbestic point of cytochrome C) and 550 nm (SpectraMax 340; Molecular Devices, Sunnyvale, CA, USA). Subsequently, the oxidative burst was initiated by the addition of 100 nM PMA. After incubation for 60 min. at 37°C the absorbance was measured. Signals were normalized to the basal readings. In addition, superoxide dismutase was added as control before PMA stimulation in selected wells. In contrast, in NOX1 transfected HEK293 cells $O_2^{\bullet-}$ was measured by luminol-enhanced chemiluminescence in white plates. For this assay HEK293 cells were transfected with NOX1, NOXO1 and NOXA1. After 48 hrs cells were removed from the flasks by trypsinization and were re-suspended in PBS. 50 µl cell suspension consisting of 100,000 cells was added in triplicate to a 96-well plate in KRPG buffer and incubated at 37ºC for 60 min. After 1 hr of incubation 50 µl reaction buffer containing 6.4 U/ml HRP and 0.4 mM luminol in KRPG buffer was added. Cells were stimulated by addition of 0.5 µM PMA. ROS generation was detected by monitoring relative light units (RLU) with a Wallac luminometer Victor2 at 37ºC for 60 min. Superoxide dismutase was added as control before PMA stimulation in selected wells.

Xanthine/Xanthine oxidase activity in cell free assays

Xanthine (X; final concentration: 50 µm) and cytochrome C (final concentration: 100 µm) were dissolved in HBSS, and 100 µL aliquots of this solution were transferred to individual wells of a 96-well plate. After addition of the oxidase inhibitors, the mixtures were allowed to equilibrate for 20 min. The reaction was started by the addition of 100 µL xanthine oxidase (XO) (final

concentration: 5 mU·mL-1), and absorbance at 540 and 550 nm was recorded 10 min. after the start of the reaction. $O_2^{\bullet-}$ production was calculated by normalization to the signals obtained at 540 nm. Similar experiments were performed with 0.4 mM luminol instead of cytochrome C. After 20 min. equilibration, the reaction was started with XOD (1 mU·mL-1), and chemiluminescence was subsequently recorded for 20 min. in a Fluoroscan FL microplate reader. Signals were calculated as AUC and normalized to the X/XOD-derived control signal. Accordingly, a counter screen has been performed with cytochrome C or luminol without X/XO-generated $O_2^{\bullet-}$.

H_2O_2 measurement in cell free system

The fluorescence of Amplex Red was measured in presence and absence of H_20_2 (0.25 µM), reflecting NOX4 and NOX5 output. After addition of inhibitors and 50 µl Amplex Red reaction mixture containing 100 U·mL-1 HRP and 10 mM Amplex Red to each well, the plate was incubated at 37°C for 10 min. Thereafter, the plate was read at excitation (530-560 nm) and emission ~ 590 nm at 37ºC and for 60 min. Data was calculated as the AUC over 60 min. and data were normalized to H_20_2 output in absence of inhibitor.

Cell permeability in HBMECs

For the passive dye diffusion assay, 2 x 10^4 human brain microvascular endothelial cells (HBMECs) were grown to confluence on membranes of Transwell inserts (collagen-coated Transwell Pore Polyester Membrane Insert; pore size = 3.0 µm (Corning, The Netherlands) Fig. 4A). After 6hrs of ischemia, cells were treated with 0,1 µM ML171, 0,6 µM VAS2870, 1 µM GKT136901, 0,2 µM M13 or 0,01 µM ML090 during 24hrs of re-oxygenation. Thereafter, cell permeability was assessed using Evans Blue (Sigma-Aldrich, The Netherlands) (Fig. 4B). First, the medium was removed and previously warmed (37°C) PBS (1,5 ml) was added to the abluminal side of the insert. Permeability buffer (0,5 ml) containing 4% bovine serum albumin (Sigma-Aldrich,

The Netherlands) and 0,67 mg/ml Evans blue dye in PBS was loaded on the luminal side of the insert followed by 15 min. incubation at 37°C. The concentration of Evans Blue in the abluminal chamber was measured by determining the absorbance of 200 µl buffer at 630 nm using a microplate reader.

Statistical analysis

Data analysis was performed using Prism 6.0g software package (GraphPad Software, San Diego, USA). IC_{50} values were calculated with a non-linear regression analysis using an algorithm for sigmoidal dose–response with variable slopes. Results are expressed as means ± SEM. Statistical differences between means were analysed by one-way ANOVA followed by Bonferroni correction for multiple comparisons. A value of $P < 0.05$ was considered statistically significant.

Results

NOX pharmacological isoform selectivity

To characterize the NOX isoform selectivity of the current second generation NOX inhibitors we determined concentration-dependency and efficacy of GKT136901, Ml171, VAS2870, M13 and ML090 on NOX1, 2, 4, and 5 (Fig. 1A). Specifically, NOX2 expressing HL-60 cells or HEK293 cells transfected with NOX1, NOX4 or NOX5 were incubated in presence of increasing concentrations of each compound. ROS generation was subsequently induced by phorbol 12-myristate 13-acetate (PMA) to stimulate NOX1, NOX2 and NOX5, which was assayed in presence of ionomycin. Thereafter, ROS production was assayed using a panel of cellular assays with structurally unrelated probes; *i.e.* Amplex red, luminol or cytochrome C (Figure 1B). Amplex red was used to quantify extracellular H_2O_2 [29], $O_2^{\bullet-}$ generation was detected by luminol-based chemiluminescence and cytochrome C-reduction was quantified to assess NOX2 activity.

NOX isoform concentration-response curves for GKT136901, Ml171, VAS2870, M13 and ML090 were constructed (Fig. 2; see table 1 for IC_{50} values). GKT136901 (Fig. 2A) showed selectivity for NOX1 over NOX4 and NOX5 inhibition while NOX2 inhibition was not observed. The same holds true for ML171 (Fig. 2B) which is more selective for NOX1 compared to NOX4 and NOX5. VAS2870 (Fig. 2C) displayed NOX2 over NOX1 and NOX4 selective inhibition and also slightly inhibited NOX5. The GlucoxBiotech compound M13 (Fig. 2D) showed almost selective NOX4 inhibition but NOX2 (with low E_{max}) and NOX1 (at high concentrations) inhibition was observed as well. Finally, Ml090 (Fig. 2E) inhibited NOX5, NOX1 and NOX4 with comparable IC_{50} but enhanced E_{max} for NOX5 inhibition. These data suggest that NOX inhibitors indeed display differential isoform targeting and therefore should be considered ideally by combined analysis of an inhibitor panel and ranking potencies.

Non-specific anti-oxidant and assay artefacts

To screen for possible assay interference between GKT136901, ML171, VAS2870, M13 or ML090 and the NOX1 assay, a cell-free system was performed in which each inhibitor was screened in presence of luminol, 1mU/ml xanthine oxidase (XO) and 1mg xanthine (X) generating $O_2^{\bullet-}$. At concentrations 1µM GKT136901 did not show interference with either the molecular probe or with the X/XO system (Fig. 3A). Similar findings were obtained with 0.1 µM ML171, 10 µM VAS2870 and 30 nM ML090 (Fig. 3A). In contrast, 1 µM M13 enhanced chemiluminescence (Fig. 3A). To identify direct interactions between assay components and GKT136901, ML171, VAS2870, M13 or ML090 a cell-free counter screen was performed without X/XO-generated ROS. Indeed, ML171 and VAS2870 showed reduction of the luminol-based signal suggesting direct interference with luminol-based chemiluminescence (Fig. 3B). In contrast, in presence of ML090 the signal was enhanced (Fig. 3B).

To study non-specific antioxidant effects of VAS2870, the effect of 10 µM VAS2870 was studied in a cell free system in presence of cytochrome C, and X/X0-derived ROS. In these assays, VAS2870 showed significant antioxidant effects (Fig. 3C).

To study whether the effects of GKT136901, ML171, VAS2870, M13 and ML090 on NOX4 and NOX5 are specific, a cell-free assay was performed with NOX4 or NOX5 effective concentrations of each inhibitor in presence of 0.25µM H_20_2 in an Amplex red assay. ML171, VAS2870, M13 and ML090 did not directly affect Amplex red-based detection of H_2O_2 (Fig. 3D). However, GKT136901 reduced Amplex red-based H_20_2 signals suggesting assay interference. Hence, the assay was repeated without H_20_2 to study potential direct assay component interference. Indeed, GKT136901, ML171, M13 and ML090 reduced the H_20_2 signal as compared to the H_20_2 control (Fig. 3E) whereas in presence of VAS2870 the signal was enhanced (Fig. 3E).

As predicted from the inhibitor screen, M13, GKT136901 or ML171 protect against ischemia-induced hyperpermeability in a human brain ischemia model. Our data suggested that a

NOX inhibitor panel may be used for target validation of specific NOX isoforms. We thus tested our NOX inhibitor panel in an *in vitro* human model of brain ischemia (Fig. 4A) where NOX4 is involved in subacute hypoxia-induced increases in cell permeability whereas NOX1, NOX2 do not [30] and NOX5 only acutely (Casas et al., unpublished observation). Primary HBMEC cultures were subjected to 6h of hypoxia followed by 24h of re-oxygenation in presence or absence of ML171 (0.1 µM; mainly targeting NOX1), VAS203 (0.6 µM; mainly targeting NOX2), GKT136901 (1 µM; mainly targeting NOX4), M13 (0.2 µM; mainly targeting NOX4) or MI090 (0.01 µM; mainly targeting NOX5). Hypoxia increased cell permeability after 24hrs of re-oxygenation. GKT136901, and ML171 treatment prevented this detrimental effect (Fig. 4C), suggesting protection against hyperpermeability via NOX4 inhibition while, as expected given their respective IC_{50} values, VAS2870, M13 or MI090 treatment showed no effect (Fig. 4C). These data provided proof-of-concept for pharmacological target validation using NOX inhibitor panels.

Discussion

Our results clearly show that using NOX inhibitor panels for isoform-selective pharmacological target validation is feasible. In this study, we provide the isoform (NOX 1, 2, 4 and 5) preferences as IC_{50} values and maximal efficacies of the currently five most advanced NOX inhibitors, GKT136901, ML171, VAS2870, M13 and ML090. We also apply some of the most commonly used ROS assays and detect for GKT136901 and ML171 relevant, non-specific antioxidant effects and assay artefacts by either interacting with the assay or directly with ROS in concentrations similar to the IC_{50} values. Highest potencies were observed for GKT136901 and ML171 with NOX1 over NOX 4 and 5, VAS2870 with NOX2 over NOX1, 4 and 5, M13 with NOX4 and ML090 with NOX5 over NOX1, 4 and 5 (table 1). None of these small molecule inhibitors are isoform selective but inhibited several NOX isoforms with different ranking potencies.

In detail, VAS2870 has been claimed a pan NOX inhibitor [31] because NOX1, 2, 4 and 5 [23,30] [32,33] activity was inhibited but only IC_{50} values for NOX2 were published [33,34]. We showed that VAS2870 is highly potent for NOX2 (IC_{50} ~ 0.7µM), followed by IC_{50} values in low micromolar range for NOX1 and 4 and higher micromolar range for NOX5 although E_{max} was higher for NOX5 than NOX4 verifying that VAS2870 is not isoform selective but inhibits all four NOX isoforms. In addition, we found that M13 is a first-in-class NOX 4 inhibitor as it is 200 times (IC_{50} ~ 0.01 µM) more potent with similar E_{max} than NOX1 (IC_{50} ~ 0.2 µM). Inhibition of NOX2 could be seen only slightly at very low concentrations (IC_{50} ~ 41 µM) and little efficacy (E_{max} ~20% inhibition) while almost no effective NOX5 inhibition could be detected at therapeutic dose. Finally, we identified Ml090, based on a quinoxaline scaffold, as a NOX5 inhibitor. So far it has been published to be active with the highest preference for NOX1 (IC_{50} ~ 25 nM) over NOX2, 3 and NOX4 with IC_{50}s of >10 µM [35]. However, in our study Ml090 was mostly inhibited NOX5 activity (IC_{50} ~ 11 nM) while similar preferences for NOX1 - and NOX4 - over NOX2 inhibition were detected as published earlier. The IC_{50}s for NOX5, 1 and 4 inhibitions are very similar suggesting Ml090 to be a pan NOX inhibitor as well, which may complicate further analysis of biochemical properties of single NOX isozymes.

While VAS2870, M13, Ml090 did not show assay interferences, the clinically most advanced compound, GKT136901, claimed to be NOX1 and 4 specific, showed direct assay interference with Amplex Red (NOX4 and 5 assay) and luminol (NOX1 assay) and ROS-scavenging effects. The latter has been verified in the alternative H_2O_2 measuring HVA assay (tested from >10µM)[36]. Likewise, non-specific antioxidant effects of GKT136901 have been published earlier such as inhibition of xanthine oxidase at high concentrations (100 µM) [37] or peroxynitrite scavenging [25]. In addition, it could also act like a peroxidase inhibitor, thus limiting application of common used ROS assays. This may thus complicate the interpretation of results regarding the contribution of NOX enzymes in disease models, questioning the proposed isoform

selective inhibition of GKT136901. In this context, the 2-acetylphenothiazine ML171 which has been published to be NOX1 specific and has xanthine oxidase activity [38], showed assay interferences with i) Amplex Red in similar NOX1 effective concentrations, with ii) the HVA assay (tested >10μM) and interfered with the iii) luminol NOX1 assay. These data are in line with a previous publication that discovered ML171 to be inactive on all NOX isoforms but interact with the Amplex red assay by either an intrinsic antioxidant activity or inhibition of horseradish peroxidase [39]; the latter would support previous observations that phenothiazines are peroxidase substrates [40]. Facing different assay problems that may limit interpretations, we suggest here to use a NOX inhibitor panel at IC_{50} concentrations for isoform-specific target validation. Importantly, we could validate this approach by GKT136901, ML171 and M13 being neuroprotective in a manner that suggested NOX4 as responsible isoform as had previously been validated genetically [13].

In summary, all tested NOX inhibitor compounds displayed different isoform profiles suggesting differential chemical targeting. This knowledge will be valuable to advance further lead optimization to allow single compound target validation with potential for progress towards specific therapeutic development. We also provide an immediately applicable inhibitor panel approach that allows target validation of NOXs under conditions where gene knock-out or knock-in is not feasible or desirable.

Acknowledgements

We wish to thank Per Wikström for providing M13, V. Jaquet for experimental advice. Financial support (to HHHWS) by the ERC (AdG RadMed and PoC SAVEBRAIN) and H2020 (REPO-TRIAL) is gratefully acknowledged.

Author Contributions

H.H.H.W.S., V.T.D and S.A. designed research; V.T.D., S.A, M.E. P.L, A.I.C and U.K performed research; V.T.D, S.A, A.I.C, M.M. and H.H.H.W.S. analyzed and interpreted data; M.M contributed in writing and revised the final manuscript and figures; V.T.D. and H.H.H.W.S. wrote and edited figures and manuscript.

Conflicts of interest

None to declare.

References

[1] Y. Dotan, D. Lichtenberg, I. Pinchuk, No evidence supports vitamin E indiscriminate supplementation, Biofactors. 35 (2009) 469–473. doi:10.1002/biof.61.

[2] E.R. Miller, R. Pastor-Barriuso, D. Dalal, R.A. Riemersma, L.J. Appel, E. Guallar, Meta-analysis: high-dosage vitamin E supplementation may increase all-cause mortality, Ann. Intern. Med. 142 (2005) 37–46. doi: 10.7326/0003-4819-142-1-200501040-00110

[3] G. Bjelakovic, D. Nikolova, L.L. Gluud, R.G. Simonetti, C. Gluud, Mortality in randomized trials of antioxidant supplements for primary and secondary prevention: systematic review and meta-analysis, Jama. 297 (2007) 842–857. doi:10.1001/jama.297.8.842.

[4] Heart Outcomes Prevention Evaluation Study Investigators, S. Yusuf, G. Dagenais, J. Pogue, J. Bosch, P. Sleight, Vitamin E supplementation and cardiovascular events in high-risk patients, N. Engl. J. Med. 342 (2000) 154–160. doi:10.1056/NEJM200001203420302.

[5] T. Finkel, Signal transduction by reactive oxygen species, J. Cell Biol. 194 (2011) 7–15. doi:10.1083/jcb.201102095.

[6] P.D. Ray, B.-W. Huang, Y. Tsuji, Reactive oxygen species (ROS) homeostasis and redox regulation in cellular signaling, Cell. Signal. 24 (2012) 981–990. doi:10.1016/j.cellsig.2012.01.008.

[7] K. Wingler, J.J.R. Hermans, P. Schiffers, A. Moens, M. Paul, H.H.H.W. Schmidt, NOX1, 2, 4, 5: counting out oxidative stress, Br. J. Pharmacol. 164 (2011) 866–883. doi:10.1111/j.1476-5381.2011.01249.x.

[8] K. Bedard, K.-H. Krause, The NOX family of ROS-generating NADPH oxidases: physiology and pathophysiology, Physiol. Rev. 87 (2007) 245–313. doi:10.1152/physrev.00044.2005.

[9] V.T.-V. Dao, A.I. Casas, G.J. Maghzal, T. Seredenina, N. Kaludercic, N. Robledinos-Anton, et al., Pharmacology and Clinical Drug Candidates in Redox Medicine, Antioxid. Redox Signal. 23 (2015) 1113–1129. doi:10.1089/ars.2015.6430.

[10] S.P. Gray, E. Di Marco, J. Okabe, C. Szyndralewiez, F. Heitz, A.C. Montezano, et al., NADPH oxidase 1 plays a key role in diabetes mellitus-accelerated atherosclerosis, Circulation. 127 (2013) 1888–1902. doi:10.1161/CIRCULATIONAHA.112.132159.

[11] J.L. Wilkinson-Berka, D. Deliyanti, I. Rana, A.G. Miller, A. Agrotis, R. Armani, et al., NADPH oxidase, NOX1, mediates vascular injury in ischemic retinopathy, Antioxid. Redox Signal. 20 (2014) 2726–2740. doi:10.1089/ars.2013.5357.

[12] S. Sorce, K.-H. Krause, NOX enzymes in the central nervous system: from signaling to disease, Antioxid. Redox Signal. 11 (2009) 2481–2504. doi:10.1089/ars.2009.2578.

[13] A.I. Casas, E. Geuss, P.W.M. Kleikers, S. Mencl, A.M. Herrmann, I. Buendia, et al., NOX4-dependent neuronal autotoxicity and BBB breakdown explain the superior sensitivity of the brain to ischemic damage, Proc. Natl. Acad. Sci. U.S.a. 23 (2017) 201705034. doi:10.1073/pnas.1705034114.

[14] J.C. Jha, S.P. Gray, D. Barit, J. Okabe, A. El-Osta, T. Namikoshi, et al., Genetic Targeting or Pharmacologic Inhibition of NADPH Oxidase Nox4 Provides Renoprotection in Long-Term Diabetic Nephropathy, J. Am. Soc. Nephrol. (2014) ASN.2013070810. doi:10.1681/ASN.2013070810.

[15] C. Geis, E. Geuss, C. Sommer, H.H.H.W. Schmidt, C. Kleinschnitz, NOX4 is an early initiator of neuropathic pain, Exp. Neurol. 288 (2017) 94–103. doi:10.1016/j.expneurol.2016.11.008.

[16] S.P. Gray, E. Di Marco, K. Kennedy, P. Chew, J. Okabe, A. El-Osta, et al., Reactive Oxygen Species Can Provide Atheroprotection via NOX4-Dependent Inhibition of Inflammation and Vascular Remodeling, Arteriosclerosis, Thrombosis, and Vascular

Biology. 36 (2016) 295–307. doi:10.1161/ATVBAHA.115.307012.

[17] C. Schürmann, F. Rezende, C. Kruse, Y. Yasar, O. Löwe, C. Fork, et al., The NADPH oxidase Nox4 has anti-atherosclerotic functions, Eur. Heart J. 36 (2015) 3447–3456. doi:10.1093/eurheartj/ehv460.

[18] C.E. Holterman, J.-F. Thibodeau, C. Towaij, A. Gutsol, A.C. Montezano, R.J. Parks, et al., Nephropathy and Elevated BP in Mice with Podocyte-Specific NADPH Oxidase 5 Expression, J. Am. Soc. Nephrol. (2013) ASN.2013040371. doi:10.1681/ASN.2013040371.

[19] J.C. Jha, C. Banal, J. Okabe, S.P. Gray, T. Hettige, B.S.M. Chow, et al., NADPH Oxidase Nox5 Accelerates Renal Injury in Diabetic Nephropathy, Diabetes. 66 (2017) 2691–2703. doi:10.2337/db16-1585.

[20] D. Pandey, A. Patel, V. Patel, F. Chen, J. Qian, Y. Wang, et al., Expression and functional significance of NADPH oxidase 5 (Nox5) and its splice variants in human blood vessels, Am. J. Physiol. Heart Circ. Physiol. 302 (2012) H1919–28. doi:10.1152/ajpheart.00910.2011.

[21] T.J. Guzik, W. Chen, M.C. Gongora, B. Guzik, H.E. Lob, D. Mangalat, et al., Calcium-dependent NOX5 nicotinamide adenine dinucleotide phosphate oxidase contributes to vascular oxidative stress in human coronary artery disease, J. Am. Coll. Cardiol. 52 (2008) 1803–1809. doi:10.1016/j.jacc.2008.07.063.

[22] S. Altenhöfer, K.A. Radermacher, P.W.M. Kleikers, K. Wingler, H.H.H.W. Schmidt, Evolution of NADPH Oxidase Inhibitors: Selectivity and Mechanisms for Target Engagement, Antioxid. Redox Signal. 23 (2015) 406–427. doi:10.1089/ars.2013.5814.

[23] S. Altenhöfer, P.W.M. Kleikers, K.A. Radermacher, P. Scheurer, J.J. Rob Hermans, P. Schiffers, et al., The NOX toolbox: validating the role of NADPH oxidases in physiology and disease, Cellular and Molecular Life Sciences : CMLS. 69 (2012) 2327–2343. doi:10.1007/s00018-012-1010-9.

[24] S. Heumüller, S. Wind, E. Barbosa-Sicard, H.H.H.W. Schmidt, R. Busse, K. Schröder, et al., Apocynin is not an inhibitor of vascular NADPH oxidases but an antioxidant, Hypertension. 51 (2008) 211–217. doi:10.1161/HYPERTENSIONAHA.107.100214.

[25] S. Schildknecht, A. Weber, H.R. Gerding, R. Pape, M. Robotta, M. Drescher, et al., The NOX1/4 inhibitor GKT136901 as selective and direct scavenger of peroxynitrite, Curr. Med. Chem. 21 (2014) 365–376. doi:10.2174/09298673113209990179

[26] J. Zielonka, G. Cheng, M. Zielonka, T. Ganesh, A. Sun, J. Joseph, et al., High-throughput assays for superoxide and hydrogen peroxide: design of a screening workflow to identify inhibitors of NADPH oxidases, J. Biol. Chem. 289 (2014) 16176–16189. doi:10.1074/jbc.M114.548693.

[27] J. Zielonka, J.D. Lambeth, B. Kalyanaraman, On the use of L-012, a luminol-based chemiluminescent probe, for detecting superoxide and identifying inhibitors of NADPH oxidase: a reevaluation, Free Radic. Biol. Med. 65 (2013) 1310–1314. doi:10.1016/j.freeradbiomed.2013.09.017.

[28] S. Wind, K. Beuerlein, T. Eucker, H. Müller, P. Scheurer, M.E. Armitage, et al., Comparative pharmacology of chemically distinct NADPH oxidase inhibitors, Br. J. Pharmacol. 161 (2010) 885–898. doi:10.1111/j.1476-5381.2010.00920.x.

[29] G.J. Maghzal, K.-H. Krause, R. Stocker, V. Jaquet, Detection of reactive oxygen species derived from the family of NOX NADPH oxidases, Free Radic. Biol. Med. 53 (2012) 1903–1918. doi:10.1016/j.freeradbiomed.2012.09.002.

[30] C. Kleinschnitz, H. Grund, K. Wingler, M.E. Armitage, E. Jones, M. Mittal, et al., Post-stroke inhibition of induced NADPH oxidase type 4 prevents oxidative stress and neurodegeneration, PLoS Biol. 8 (2010) e1000479. doi:10.1371/journal.pbio.1000479.

[31] K. Wingler, S.A. Altenhoefer, P.W.M. Kleikers, K.A. Radermacher, C. Kleinschnitz,

H.H.H.W. Schmidt, VAS2870 is a pan-NADPH oxidase inhibitor, Cellular and Molecular Life Sciences : CMLS. 69 (2012) 3159–3160. doi:10.1007/s00018-012-1107-1.

[32] R. Bretón-Romero, C. González de Orduña, N. Romero, F.J. Sánchez-Gómez, C. de Álvaro, A. Porras, et al., Critical role of hydrogen peroxide signaling in the sequential activation of p38 MAPK and eNOS in laminar shear stress, Free Radic. Biol. Med. 52 (2012) 1093–1100. doi:10.1016/j.freeradbiomed.2011.12.026.

[33] G.J. Gatto, Z. Ao, M.G. Kearse, M. Zhou, C.R. Morales, E. Daniels, et al., NADPH oxidase-dependent and -independent mechanisms of reported inhibitors of reactive oxygen generation, J Enzyme Inhib Med Chem. 28 (2013) 95–104. doi:10.3109/14756366.2011.636360.

[34] H. ten Freyhaus, M. Huntgeburth, K. Wingler, J. Schnitker, A.T. Bäumer, M. Vantler, et al., Novel Nox inhibitor VAS2870 attenuates PDGF-dependent smooth muscle cell chemotaxis, but not proliferation, Cardiovasc. Res. 71 (2006) 331–341. doi:10.1016/j.cardiores.2006.01.022.

[35] S.J. Brown, D. Gianni, G. Bokoch, B.A. Mercer, P. Hodder, H.R. Rosen, Probe Report for NOX1 Inhibitors, (2010).

[36] K.D. Martyn, L.M. Frederick, K. von Loehneysen, M.C. Dinauer, U.G. Knaus, Functional analysis of Nox4 reveals unique characteristics compared to other NADPH oxidases, Cell. Signal. 18 (2006) 69–82. doi:10.1016/j.cellsig.2005.03.023.

[37] M. Sedeek, G. Callera, A. Montezano, A. Gutsol, F. Heitz, C. Szyndralewiez, et al., Critical role of Nox4-based NADPH oxidase in glucose-induced oxidative stress in the kidney: implications in type 2 diabetic nephropathy, Am. J. Physiol. Renal Physiol. 299 (2010) F1348–58. doi:10.1152/ajprenal.00028.2010.

[38] D. Gianni, N. Taulet, H. Zhang, C. DerMardirossian, J. Kister, L. Martinez, et al., A novel and specific NADPH oxidase-1 (Nox1) small-molecule inhibitor blocks the formation of functional invadopodia in human colon cancer cells, ACS Chem. Biol. 5 (2010) 981–993. doi:10.1021/cb100219n.

[39] T. Seredenina, G. Chiriano, A. Filippova, Z. Nayernia, Z. Mahiout, L. Fioraso-Cartier, et al., A subset of N-substituted phenothiazines inhibits NADPH oxidases, Free Radic. Biol. Med. 86 (2015) 239–249. doi:10.1016/j.freeradbiomed.2015.05.023.

[40] T.V. Rogozhina, V.V. Rogozhin, [Phenothiazines are slowly oxidizable substrates of horseradish peroxidase], Biomed Khim. 57 (2011) 544–553. https://doi.org/10.1134/S1990750811040093

Tables

Table 1: IC_{50} values for NOX isoform inhibition.

	NOX1	NOX2	NOX4	NOX5
GKT136901 (μM)	0.7	> 1000	1.1	0.7
ML171 (μM)	0.1	6.9	0.6	0.6
VAS2970 (μM)	4.2	0.7	5.6	20.5
M13 (μM)	0.2	40.9	0.01	125
ML090 (nM)	25	> 1000	20	10.8

Figure legends

Figure 1: Chemical structures. Chemical structure of NOX inhibitors (a) and probes (b) used in the study.

Figure 2: NOX inhibitors display isoform selectivity. ROS production was assessed in whole cels using assays measuring ROS prduction by NOX1 (luminol assay, black), NOX2 (cytochrome C assay, green), NOX4 (amplex red assay, red) or NOX5 (amplex red assay, blue). As illustrated in the figure (A-E), GKT136901 (A), ML171 (B), VAS2870 (C), M13 (D) or ML090 (E) inhibited ROS production with NOX isoform specific IC_{50}. Data are presented as the mean±SEM; All ROS measurements were performed in triplicate in at least three independent experiments.

Figure 3: Several inhibitors display inhibit ROS assays. A/B) GKT136901 and VAS2870 inhibit luminol-based assays. To study possible interference of GKT136901, ML171, VAS2870, M13 or ML090 with luminol-based measurements cell-free luminol assays were used. In these assays, ROS production generated by X/XO was enhanced by M13 (A) but not by GKT136901, ML171, VAS2870 or ML090. Moreover, chemiluminescence produced by luminol only was inhibited by ML171 and VAS2870, enhanced by ML090 and not affected by GKT136901 or M13, respectively (B). C) Possible assay interference by NOX2-specific VAS2870 was assessed by studying cytochrome C reduction in presence of X/XO-derived ROS in a cell free system. Presence of VAS2870 slightly, but significantly reduced chemiluminescence. D/E) The possibility of interference between GKT136901, ML171, VAS2870, M13 or ML090 and Amplex Red-based assays was studied using cell-free Amplex Red assays. In these assays, ROS production generated by H_2O_2 was inhibited by GKT136901 (D) but not by ML171, VAS2870, M13 or ML090 (D). Moreover, fluorescence produced by Amplex Red only was inhibited by GKT136901, ML171, M13

and ML090 while it was enhanced by VAS2870 (E). Data are presented as the mean±SEM; All ROS measurements were performed in triplicate in at least three independent experiments.

Figure 4: GKT136901, GKT136901 and M13 inhibit ischemia-induced hyperpermeability. HCMECs were subjected to 6hrs ischemia followed by 24hrs re-oxygenation during which inhibitors were present. Cell permeability was subsequently assessed by measuring Evans Blue (EB) fluorescence. Ischemia cause hyperpermeability (black bar) which was significantly reduced in cells treated with ML171 (0.1 μM) or GKT136901 (0.1 μM) while M13 (0.2 μM), VAS2870 (0.6 μM) or ML090 (0.01 μM) treatment had no effect. Data are presented as the mean±SEM; * $P < 0.05$. n = 5/6.

Figure 1

A

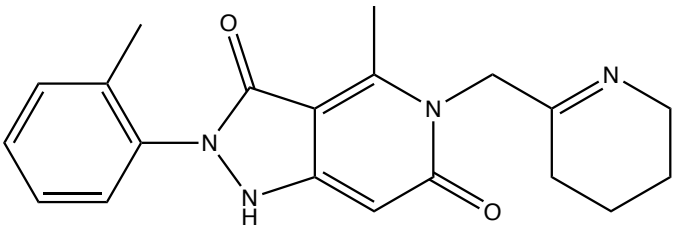

GKT136901

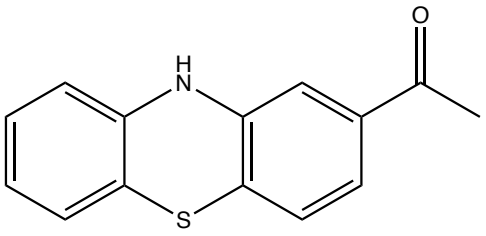

ML171

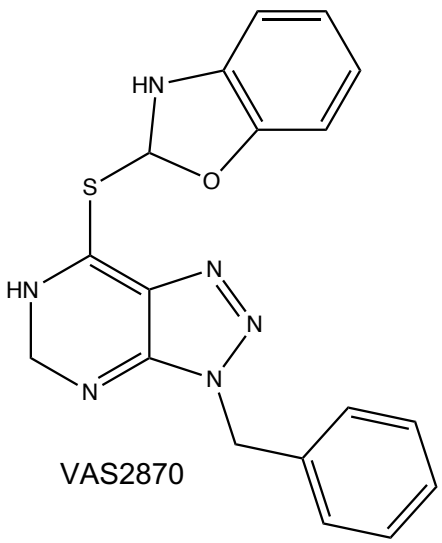

VAS2870

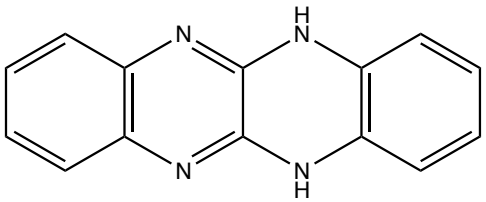

ML090

B

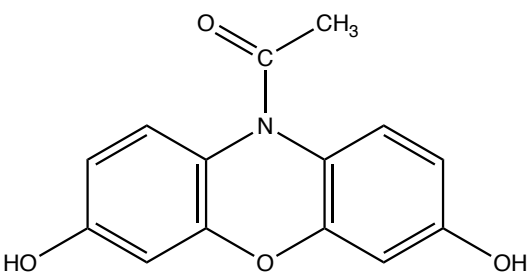

Amplex Red

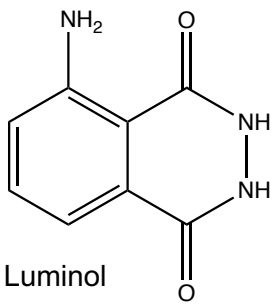

Luminol

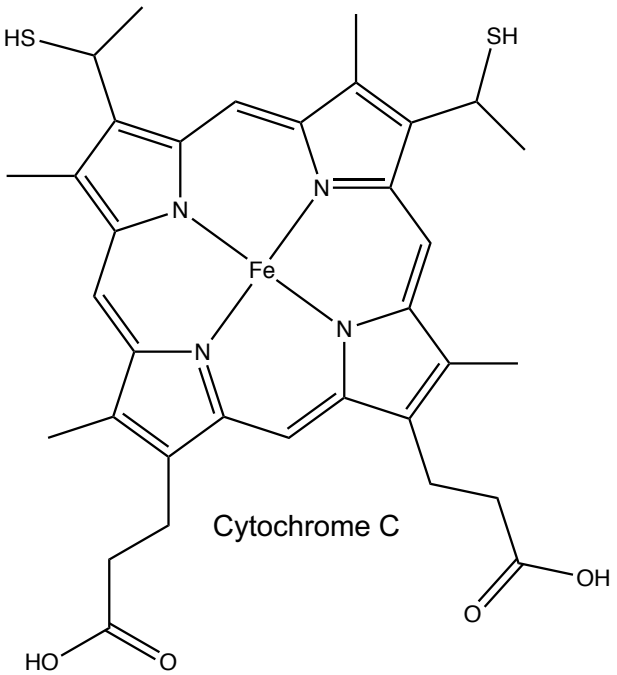

Cytochrome C

Figure 2

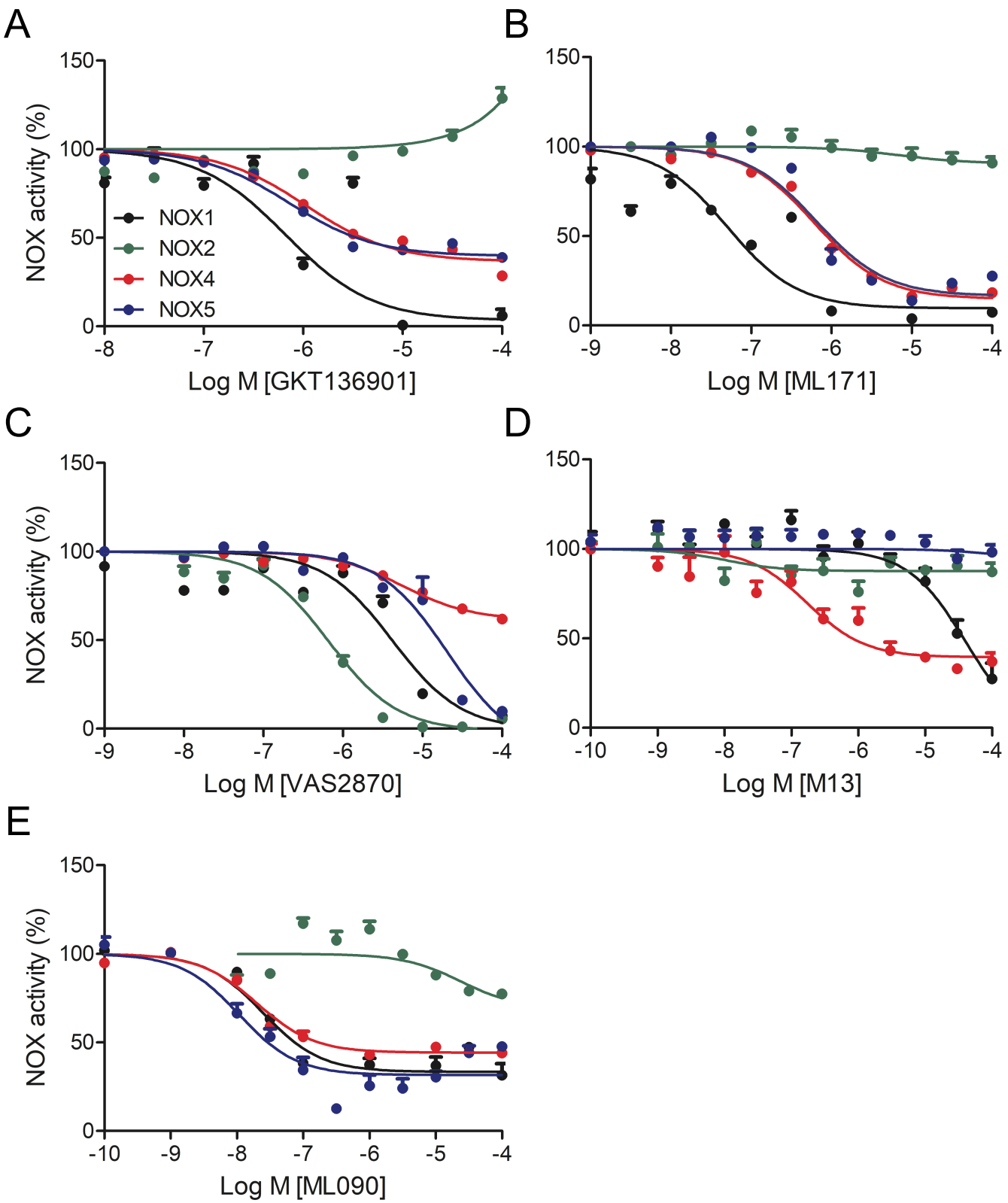
A
B
C
D
E
NOX activity (%)
NOX1
NOX2
NOX4
NOX5
Log M [GKT136901]
Log M [ML171]
Log M [VAS2870]
Log M [M13]
Log M [ML090]

Figure 3

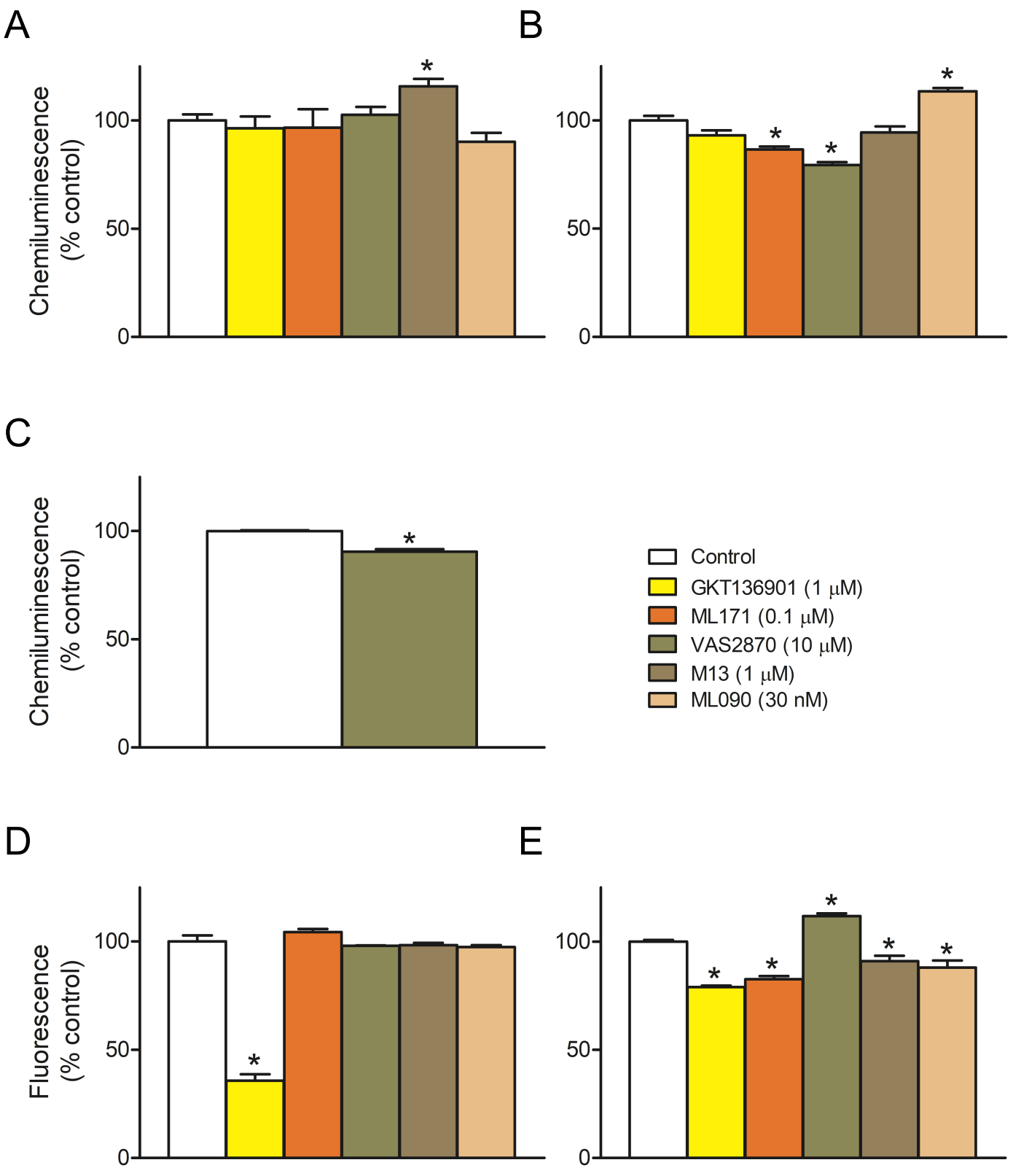
A
B
C
D
E
Chemiluminescence (% control)
Fluorescence (% control)
100
50
0
*
Control
GKT136901 (1 μM)
ML171 (0.1 μM)
VAS2870 (10 μM)
M13 (1 μM)
ML090 (30 nM)

Figure 4

A

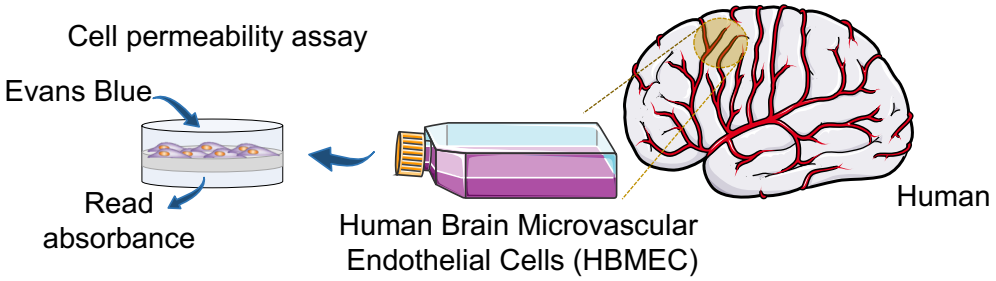
Cell permeability assay
Evans Blue
Read absorbance
Human Brain Microvascular Endothelial Cells (HBMEC)
Human

B

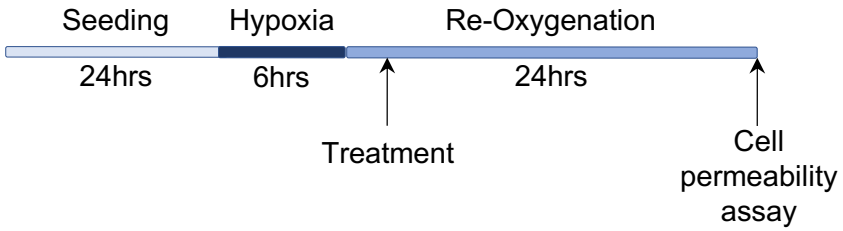
Seeding
Hypoxia
Re-Oxygenation
24hrs
6hrs
24hrs
Treatment
Cell permeability assay

C

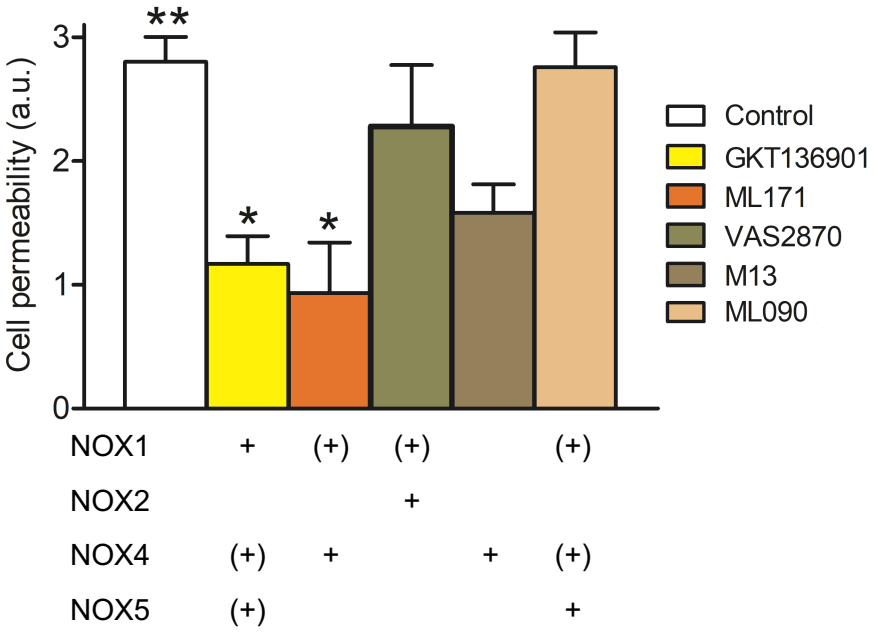
Cell permeability (a.u.)
0
1
2
3
**
*
*
Control
GKT136901
ML171
VAS2870
M13
ML090
NOX1 + (+) (+) (+)
NOX2 +
NOX4 (+) + + (+)
NOX5 (+) +